EXPERIMENTAL INVESTIGATION OF CRITICAL HEAT FLUX FOR ZERO AND NATURAL CIRCULATION FLOW OF WATER IN THREE RODS BUNDLE NEAR ATMOSPHERIC PRESSURE

Y. Aharon[1,2], I. Hochbaum[1]
[1]: NRCN, P.O.Box 9001 Beer Sheva, Israel
[2]: Department of Mechanical Emgineering, Ben Gurion University, P.O.Box 653
Be'er Sheva, Israel, 8410501
Email: jaharon@post.bgu.ac.il

ABSTRACT

The present work deals with Critical Heat Flux (CHF) phenomenon in three rods bundle inside a round channel. The experiments was conducted at zero and natural circulation conditions. Those conditions may be the nominal design cooling conditions of advanced small reactors or the condition in case of cooling channel blockage accident. In case of a vertical narrow and long heated channel with stagnant or low flow rate, the mechanism which limiting the maximum heat flux is a countercurrent flow between the vapor which flows in the upper direction and the water which flows in the other direction. In this paper, the experiments performed with water in a three rods bundle 12 mm in diameter and 1000 mm in length. The rods locater inside a Pyrex channel 31 mm in diameter. The rods bundle was in a triangle arrangement with p/d=1.17. The experiments conducted in a closed inlet valve condition and in open valve and natural circulation mode. In the first case, the subcooling range was between 40-80 ^{o}C while in the natural circulation the subcooling was varied during the experiment due to the water reservoir heating. The experimental CHF results compared with known correlations and some deviation was observed.

KEYWORDS: rod bundle, critical heat flux, natural circulation

1. INTRUDUCTION

In the last half century, extensive experimental and theoretical works have been performed on boiling Critical Heat Flux (CHF) phenomena. CHF is a condition in which a small increase in heat flux leads to abrupt wall overheating, caused by the transition or Departure from Nucleate Boiling (DNB) to film boiling. Much effort was devoted to understand the phenomena and to develop design predicting correlations. Since the foregoing studies are mostly related to nuclear power plants, most of the existing experimental data, are at a high pressure (say 2.5-20.0 Mpa) and high flow velocity and so are the correlations which have been developed. Other works in the literature tried to understand the pool boiling CHF mechanism which characterizes by a natural convection driving force and very low velocities.

The last nuclear accident in Fokushima which was a result of electrical supply failure due to the Tzunami, was a trigger for researches on cooling accidents in nuclear reactors. In case of Loss Of Coolant Accident (LOCA) or Loss Of Flow Accident (LOFA) in nuclear power plains or in a research reactors the flow velocity and / or the pressure decreases. In this case, the CHF in the fuel channels is occurring due to another mechanism which differs from the pool boiling or forced convective flow boiling CHF. The understanding of the fundamental nature of that kind of CHF in vertical flow channel under stagnant or low flow conditions is important for reactor safety.

In a case of vertical channel with a large liquid volume, the CHF mechanism is similar to the Departure from Nucleate Boiling (DNB) in pool boiling. When the vertical heated channel becomes narrow and long like in a fuel channel, the CHF mechanism, which limiting the residual heat removing from the fuel, calls Flooding CHF. In this mechanism, a countercurrent flow is formed in the vertical flow channel by the vapor which flows in the upper direction and the water which flows in the other direction due to the gravitation. Several investigators (Mishima and Nishihara [1], El- Genk et al. [2], Chang et al. [3], Park, J. W. et al. [4] and S-Y. Chun et al. [5]) have conducted experiments under those conditions of stagnant or low flow rate between zero to several hundred kg m^{-2} s^{-1}. Mishima conducted his experiment with one side heated annular

channel and with rectangular channel and round tube. He compared his results with several correlations and found that the best prediction of the experimental results was achieved with his correlation which was a modification of Wallis correlation:

$$q^* = q^*_{cF} + \frac{A}{A_H}\frac{\Delta h_i}{h_{fg}} G^* \tag{1}$$

The second term on the r.h.s of eq. 1 is the contribution of the enthalpy increase to the saturation condition of water and the first term is the heat flux in the CHF condition under flooding in the saturation condition as follow:

$$q^*_{cF} = \frac{A}{A_H}\frac{C_w{}^2\sqrt{D^*}}{\left[1+\left(\rho_g/\rho_l\right)^{0.25}\right]^2} \tag{2}$$

In eq. 2, $G^* = G\Big/\sqrt{\lambda\rho_g g\Delta\rho}$ and $q^* = q\big/h_{fg}\sqrt{\lambda\rho_g g\Delta\rho}$. Mishima reported that the flooding CHF was well reproduced with C_w=1.66, 0.98 and 0.73 for tubes annuli and rectangular channels respectively. Equation 1 presents the CHF in case of low flow rate which is a superposition of the Flooding CHF (eq. 2) and the influence of the flow rate (G*). The fact that C_w in equation 2 has different value for each channel geometry presents a problem to generalized that equation for every geometry by using a dimensionless groups. The difference between the calculated values for tubes annuli and rectangular channels with the same D_{hy} and heating area and flow cross section may reach a factor of 5.
Several investigators have employed Kutateladze's criterion for the onset of flooding given by the following expression:

$$K_g^{0.5} + mK_l^{0.5} = C_k \tag{3}$$

Where K_g and K_l are defined by: $K_i = j_i\rho_i^{0.5}(g\sigma\Delta\rho)^{-0.25}$ (The subscript i=l or i=g for liquid or vapor respectively). C_k and m are constant which were defined by Pushkina and Sorokin [6] as m=0 and C_k^2=3.2 for flooding conditions. Tien and Chung [7] took m=1 in eq. 3 and after substitution j_g and j_l they got the following expression:

$$\frac{q_{C,B}}{h_{lg}\left(g\sigma\rho_g^2\Delta\rho\right)^{1/4}} = \frac{C_k^2}{4}\left(\frac{D_{he}}{L_B}\right)\left[1+\left(\frac{\rho_g}{\rho_l}\right)^{1/4}\right]^{-2} \tag{4}$$

They defined the constant C_k as a function of Bond number Bo as follows: $C_k^2=3.2[\tanh(Bo^{1/4}/2)]^2$.

El- Genk et al.[2] conducted experiments with an annular transparent test section which was heated from the inner wall. The heater length was 500 mm and its outer diameter was 12.7 mm. The ratio between the annulus inner and outer diameter was ε=1.575 to 2 which gives a length to diameter ratio between 39 and 68. They observed that the flooding CHF occurs in the zone of the annular and the churn flow regime. They compared their and Mishima's experiment data with known correlations of flow boiling CHF such as Biasi et al. [8], Macbeth [9] and Bernath [10] correlations and they found a bad agreement between them includes the results in zero flow rate conditions. The correlation of both Biasi and Macbeth predict zero CHF values for zero flow conditions, results which were in contrast with their experimental data. Extrapolation of the Bernath correlation to a low flow conditions overestimates the CHF prediction in about one order of magnitude in comparison with the experimental data. They developed a new correlation for low flow rate which was in a good agreement with their results as follows:

$$q^*\left(\frac{A_h}{A}\right) = 1.65\left[\frac{L}{D_{eh}}\right]^{0.2}\left[0.933 + 0.212\frac{G^*\Delta h_i}{h_{fg}}\right] \tag{5}$$

That correlation fitted well the results of the experiments with annular channel between ε=1.72 to 2.0. In a smaller diameters ratio of ε=1.575 they need another correlation. For zero flow rate they used Walis's correlation (eq. 2) and found that that correlation underpredicts their experimental results but the best agreement was achieved with C_w^2=1 which gave underprediction of about 10%.

S. Y. Chun et al. [5] conducted experiments with higher values of heated length to hydraulic diameter ratio. Their test section was consisted of a vertical annular flow channel with upper and lower plenums. The annulus flow channel was 9.54 and 19.4 mm inner and outer diameters respectively and a heated length of 1842 mm (L/D=186). They also conducted experiments with non uniform heat flux distribution along the heated channel with the same geometry. The length of the channel and the power distribution in this case are much closer to the geometry and operation condition of fuel channel in a nuclear power plane. Comparison of their experimental results with Mishima and Nishihara correlation (eq. 2) show a large scatter in both heat flux distributions. On the other hand, comparison of the experimental results with Kutatelatze correlation and taking C_k^2=3.2, without the function of Bo number, show a good agreement.

In later paper of Seok Cho et al. [11], they conducted experiments on CHF under zero flow conditions with non uniformly heated 3x3 rod bundle. The heated length of the rods was 3.73 m and the rods outer diameter and the pitch were 9.52 mm and 12.6 mm respectively. Those experiments were conducted in a pressure range between 0.5 to 14.96 MPa. They found that the CHF occur in the upper region of the heated section but that location move gradually in downward direction with increasing of the system pressure. Comparison of the experimental results with Mishima's correlation (eq. 2) show a good agreement when they took C_w^2 as follow:

$$C_w^2 = 1.22\left(\frac{L_B}{D_{he}}\right)^{0.12}\left(\frac{\rho_g}{\rho_l}\right)^{0.064}\left(1+0.055Bo-4.08\text{x}10^{-3}Bo^2\right) \tag{6}$$

A good agreement was also achieved by using Nejat [12] correlation and using eq. 6 for C_w^2 :

$$\frac{q_{C,B}}{h_{\text{lg}}\rho_g\left(gD_{hy}\right)^{1/2}} = \frac{C_w^2}{4}\left(\frac{D_{he}}{L_B}\right)\left(\frac{\Delta\rho}{\rho_g}\right)^{0.5}\left[1+\left(\frac{\rho_g}{\rho_l}\right)^{1/4}\right]^{-2} \tag{7}$$

As it was presented above most of the experimental works on flooding CHF used annular or rectangular channels. Those researches are related to research reactor which most of them are using plats fuel element and are operating near atmospheric pressure. In nuclear power plants, the most common fuel geometry is rods bundle and the operating pressure is near 15 MPa. However, in case of LOCA it is possible that the pressure will decrease, a parameter which influences the researched flooding CHF phenomena. The present paper is a part of research which conducted to study that phenomenon in rod bundle near atmospheric pressure. In a previous paper (Y. Aharon, [13]), preliminary experimental research was conducted with a triangle rode bundle and small value of L/D_{hy}. The objective of the present study is to present preliminary results of CHF experiments in stagnant flow condition and to exam the natural circulation behavior in two phase flow conditions. The experiments carried out with a triangle rode bundle with realistic values of L/D_{hy} related to fuel elements in nuclear power plants.

2. EXPERIMENTAL EQUIPMENT

The test loop is presented in figure 1(a). The loop consists of test section, upper reservoir, water tank and circulating pump. Two valves (V2 and V3) are locating along the natural circulation loop to control the flow loop friction losses. Thermocouples were located at the inlet and the exit of the test section and also in the upper reservoir and in the water tank. Pressure drop was measured along the test section during the experiments for average void evaluation in the two phase flow conditions.

The test section was made up of three 12- mm OD, stainless steel tubes, which located inside a Pyrex tube 31 ID. The heating tubes were arrange in triangle arrangement with p/d= 1.17 where p is the pitch between the rods center and d is the rod diameter. Copper electrodes were silver soldered to each end of the stainless steel tubes. The length of the heated zone was 1000 mm as shown in Figure 1(b). Thermocouples attached to

the outside surface of two heating rods (rod 1 and 2) in various locations to measure the rods wall temperatures. The temperature measurement location in each rod presented in table I. The test section was heated electrically by a low voltage D.C power supply of 15 V and 5000 A. The power of the test section was measured by measuring the voltage and the current through the test section. The current was measured by using a calibrated shunt which located in serial with the test section.

Table I: Temperature measuring location from the bottom of the heating zone in rod #1 and #2 (in mm)

Rod 1	Rod 2
60	
300	300
500	
700	700
940	940

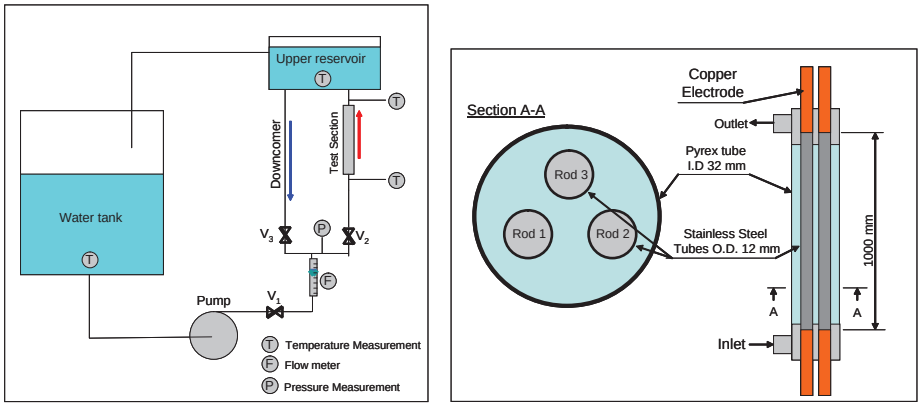

Figure 1. The test loop (a) and the test section (b)

In the natural circulation experiments, the flow-rate through the test section was calculated by using an energy balance based on the inlet and the outlet water measured temperatures and the channel power. That flow rate evaluation is correct only when the exit temperature is in subcooled condition and no vapor is flowing in the exit temperature measuring location. In the natural circulation experiments, the water from the test section flow to the upper reservoir and from the reservoir returned back in the downcomer to the channel inlet. Because of the limited water volume in the upper reservoir, during the natural circulation experiments, the reservoir temperature was increased gradually and so the inlet temperature to the test section. The pressure in the loop was always near atmospheric by keeping the water tank open to the atmosphere.

3. TEST PROCEDURE

3.1 Zero Flow experiments

The experimental procedure consisted of the following steps. The water in the water tank was heated to the required temperature. When the required temperature was achieved, the circulating pump was used to feel the test loop and the upper reservoir. The inlet valve V2 closed and at those conditions power applied to the test section and increased at small increments. After each increment, the wall temperature rose and reached a steady state and than another increment of power was applied, until the critical heat flux occurred. When the boiling started inside the test section, the measured heaters temperature reached the saturation temperature and fluctuated around that temperature. The occurrence of burnout was observed when the heater wall changed its color to red due to overheating in any location along the heaters. If the overheating of the heater

is in the vicinity of the thermocouple a sharp increasing of the measured temperature was observed. Whenever the CHF was detected, the heater power was reduced or tripped to prevent any damage to the heaters.

The CHF was calculated from the voltage drop across the test section and the electrical current, assuming a uniform heat flux. Various tests were performed for different upper reservoir temperatures. During all runs the following values were monitored (by digital and/or analog instruments):

- Temperature of water and test section in various points.
- Pressure drop.
- Electrical current and voltage.

Each run was terminated when a sudden increase of wall temperature was observed.

3.2 Natural circulation experiments

The experimental procedure in this section is almost the same as the zero flow experiments but in the natural circulation experiments the inlet valve V2 was open during the experiment. Power applied to the test section and increased at small increments. After each increment, the wall temperature rose and reached a steady state and than another increment of power was applied, until the critical heat flux occurred. During those experiments the upper reservoir temperature was increase gradually because of the limited water volume in the loop. The inlet and outlet measured temperatures were used for mass flow rate calculation through the test section. Various tests were performed for different upper reservoir initial temperatures. The in all of the experiments the exit temperature reached the saturation temperature.

4 RESULTS AND DISCUSSIONS

4.1 Zero Flow experiments

Figure 2 shows the inlet and exit water temperatures in a typical zero flow experiment. As it can be seen, in the figure, the inlet temperature is constant during the experiment and not influenced by the channel power and the increasing of the exit temperature. The exit temperature increasing gradually with the channel power up to the saturation temperatures. There are few fluctuations on that measured temperature due to the cold water which entering the channel from the upper reservoir.

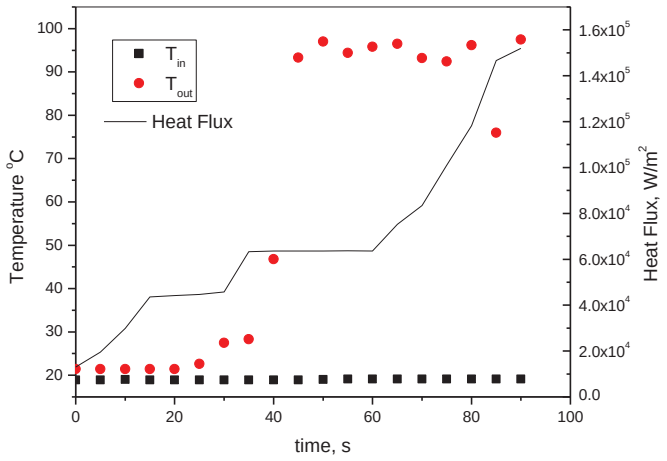

Figure 2. Heat flux, inlet and exit measured temperatures vs. time (T_{in}=20 ºC)

Figure 3 shows the rods wall measured temperatures and it can be seen that the walls temperatures increase monotonically even that the channel power is increases by steps. That behavior can be explain by the transient developing of the natural convection flow and temperatures. The walls temperatures reach the saturation temperature and continue on that value up to the channel power which creating the Critical Heat Flux (CHF). That heat flux can be observed in the figure by a sharp increasing of the wall temperature. The boiling regime which was observed inside the channel started with a bubbly flow while during the power increasing the flow regime changed to churn and annular flow. In this boiling regime, the burnout of the heating rods was observed by changing the local rods color to red. It can be seen that the temperature increasing appeared in both rod #1 and #2 in the same level (0.7 m from the bottom of the heated zone). The heat flux at that time is 100 kW/m^2. The level of the burnout along the channel was increased with increasing the inlet temperature and in 55 ^{o}C inlet temperature the burnout was observed firs in the level of 0.9 m.

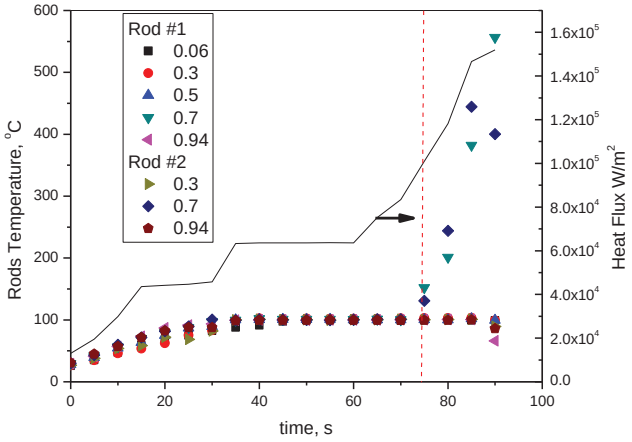

Figure 3. Heat Flux and Measured wall temperature vs. time

In figure 4 the average void fraction in the channel is presented versus the time. The average void fraction inside the channel was calculated based on the pressure drop which measured along the channel. During the experiment there is no net flow rate through the channel and the measured pressure drop is just due to the hydrostatic head. From that pressure drop, the average density inside the channel was calculated and the average void fraction. It can be seen that as long as the exit temperature is lower the saturation temperature the void fraction inside the channel is almost zero. When the exit temperature reaches the saturation value the void fraction increases. As it can be seen, before reaching the tow phase regime the void fraction is almost zero but in a heat flux of about 60 kW/m^2, the void fraction increases and reaches a value of about 50%. In that void fraction the exit temperature from the channel increases to the saturation value.

Figure 5 summarizing the experimental CHF values versus the inlet water temperature. It can be seen that the CHF values decrease with the inlet temperature in a small slope. A comparison of the experimental results with various correlation show a large scattering between the experimental results and the predicted values. It can be also observed that Mishima's correlation (eq. 2) gives a different results for various geometries (tube, annulus and rectangular channel) while the experimental values lays between the three different geometries calculated values. A good agreement was achieved between the correlation of Mishima for tube geometry and the correlation of El Genk (eq. 5) only at low inlet temperature. Better agreement was achieved with El-Genk correlation (eq. 7). That disagreement between the experimental values and the calculated values based on Mishima's correlation reported by Y. Aharon (2010) which conducted experiments with the same channel cross section and smaller L/D_{hy}.

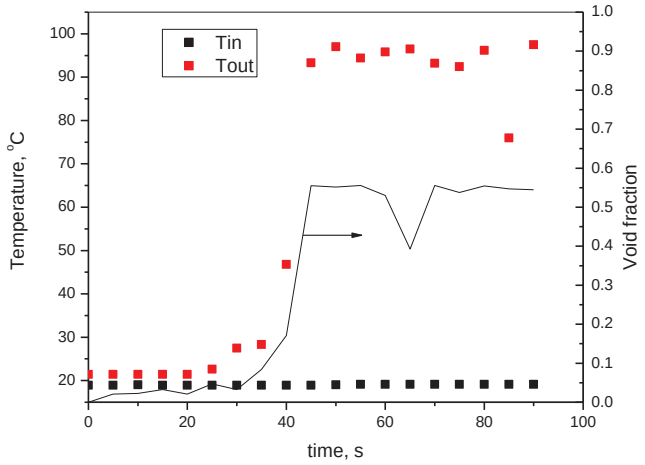

Figure 4. Void fraction, inlet and exit measured temperatures vs. time (T_{in}=20 °C)

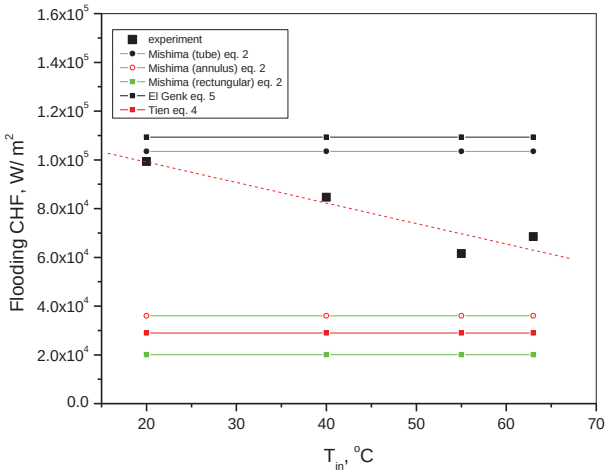

Figure 5. Comparison between measured CHF and prediction of various correlations for zero flow rate.

4.2 Natural Circulation experiments

The behavior of the heated channel during the natural circulation experiments is completely different from the zero flow rater case. In figure 6, the heat flux, the inlet and exit water temperatures are presented versus time. Those results are of a typical natural circulation experiment while the initial inlet temperature is 20 °C. As it can be seen, the inlet temperature and the exit temperature increase while the channel power is increase and that due to the finite water volume in the upper reservoir. Looking on the flow regime inside the test section one can see that at low channel power the flow inside the channel is one phase and when the power is increased, the flow regime changed to bubbly and than to slug or churn flow. In figure 6 the temperature difference between the inlet and the exit of the channel is also presented. The temperature difference between the inlet and the exit of the channel is a function of the channel power and the mass flow rate. As it can be seen, that temperature difference is increasing with the time (and the channel power) up to a maximum point and than started to decreas. The fact that the channel power was increased monotonously during the experiment, the behavior of the temperature difference can be related to a sharp increasing of the mass flow

rate due to a two phase mixture that decreasing the average channel density and increasing sharply the buoyancy driving force.

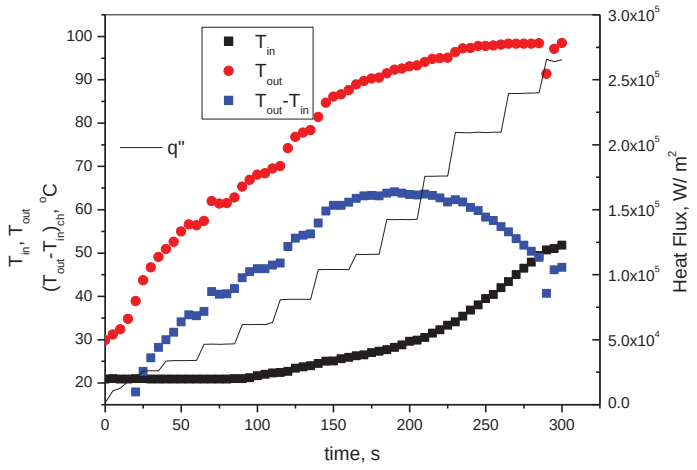

Figure 6. Heat flux, inlet and exit measured temperatures vs. time ($T_{initial}$=20 ºC)

To improve that assumption a natural circulation model was used to calculate the flow rate through the experimental loop by using the assumption of one phase flow only. It was assumed that the friction and local losses are proportional to the volumetric flow rate in power of 2. The proportionality constant was calculated based on the beginning measured points where the flow is density (which is the inlet density) and the channel average density.

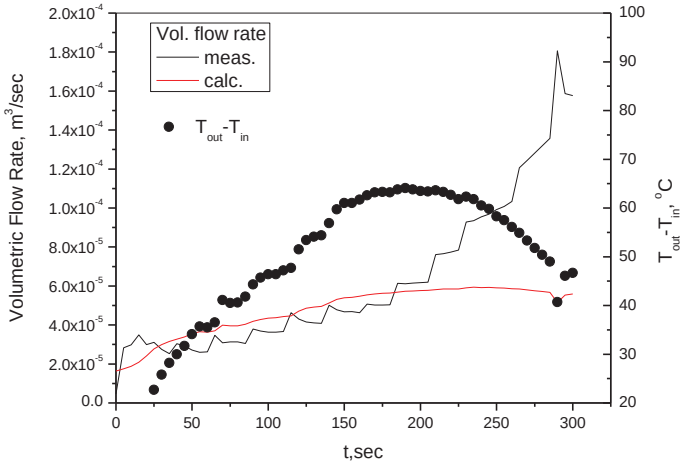

Figure 7. Comparisson between "one phase" model calculated volumetric flow rate and measure values($T_{initial}$=20 ºC)

The density based on the measured inlet and exit channel temperatures. In figure 7, a comparison between that calculated "one phase" volumetric flow rate and the measured flow rate. The last flow rate was calculated based on energy balance on the heated channel. In the figure, the temperature difference between the inlet and the exit of the channel is presented. It is very clear in the figure that the maximum point of the

temperature difference is at the point in which the flow rate started to increase sharply probably due to the bubbles creation inside the channel which causing a sharp decreasing in the channel density and increasing the buoyancy driving force. That statement should be improve by using a direct flow rate measurement, but by measuring just the inlet and the exit temperature one can identify the beginning of significant subcooled two phase flow inside the channel. The maximum heat flux that was used during the natural circulation experiments was limited by the power generator and the electrical rods resistance. Nevertheless, the exit temperature in all of the experiments reached the saturation value (zero subcooling) and two phase flow was observed inside the channel and in high channel power the flow started to oscillate. During all those experiments the system reached a maximum heat flux of 265 kW/m^2 without getting a burnout in any point along the rods.

5. CONCLUSIONS

The CHF experiments have been carried out to study the behavior of the counter current and flooding boiling limitation in triangle rod bundle inside a round channel at an atmospheric pressure in zero flow rate. The test section was connected to an upper water reservoir and the range of the water subcooling inside the reservoir was between 30 to 60 ^oC. The CHF was defined by a sudden increasing of the rods temperature and by local changing visual observation of the rods color to red. The location of the burnout was changed with the inlet (reservoir) temperature. In a high subcooling the burnout was observed at about 0.3 m from the channel exit while in a higher temperature (55 ^oC and up) the burnout started at the exit level. From a visual observation and from pressure drop measurements along the channel, the average void fraction inside the channel when the CHF occure was about 28%. The CHF values varied with the inlet subcooling while in the high subcooling the CHF value was about 100 kW/m^2 and in the lowest subcooling the CHF value decreased to about 65 kW/m^2. Comparison of the experimental results with various correlation show that the experimental results lay between the predicted values of the correlations for various geometries (Annular rectangular and round tube).
In the natural circulation experiments the inlet and the outlet temperatures varied during the experiments up to the saturation exit temperature. The maximum heat flux wich supplied to the test section reached up to 265 kW/m2 and up to that value CHF was NOT observed in the channel. It was found that from the inlet and outlet measured temperatures one can recognize the beginning of the tow phase subcooled natural circulation flow. That result is a simple tool for that observation and can be use in high pressure experiments while transparent channel is imposible.

6. REFERENCES

1. K. Mishima, H. Nishihara, Effect of channel geometry on critical heat flux for low pressure water, Int. J. Heat Mass Transfer, vol. 30, No. 6, pp. 1169-1182, (1987)
2. M. S. El-Genk, S. J. Haynes, S-H. Kim, Experimental studies of critical heat flux for low flow rate of water in vertical annuli at near atmospheric pressure, Int. J. Heat Mass Transfer, vol. 31, No. 11, pp. 2291-2304, (1988)
3. S.H. Chang, W.P. Baek and T.M. Bae, "A study of Critical Heat Flux for low Flow of Water in Vertical Round Tube under Low Pressure", Nucl. Eng. Des., 132, pp 225-237, (1991)
4. C. Park, W.P. Baek and S. H. Chang, "Countercurrent Flooding Limited Critical Heat Flux in Vertical Channels at Zero Inlet Flow", Int. Commun. Heat Mass Transfer, 24, pp.453-464, (1997)
5. S. Y. Chun, S.K. Moon, H.J. Chung, S.K. Yang, M.K. Chung, M. Aritomi, "Critical Heat Flux under Zero Flow Condition in Vertical Annulus with Uniformly and Non-Uniformly Heated Section", Nucl. Eng. Des., 205, pp. 265-279, (2001)
6. O. L. Pushkina, Y. L. Sorokin, "Breakdown of Liquid Film Motion in Vertical Tubes", Heat Transfer Soviet Res., 1, pp. 56-64, (1969)
7. C. L. Tien and K. S. Chung, "Entrainment Limits in Heat Pipes", AIAA J., 17, pp. 643-646, (1979)
8. L. Biasis, G. C. Clerici, S. Garribba, R. Sala and A. Tozzi, Stadies on burnout , part 3-A new correlation for round ducts and uniform heating and its comparison with world data, Energia Nucleare XIV(9), pp. 530-536, (1967)
9. R. V. Macbeth, Burnout analysis, Part 4- Application of local conditions hypothesis to world data for uniformly heated round tubs and rectangular channels, AEEW-R267, 1963

10. L. Bernath, A theory of local boiling burnout and its application to existing data, Chem. Engng. Prog. Symp. Ser 56, pp. 95-116, (1960)
11. S. Cho, S-Y, Chun, S-K. Moon, W-P, Beak, Y. Kim, "Flooding limited CHF in a vertical 3x3 rod bundle with non- axial heat flux", Nucl. Eng. Des., vol. 235, pp. 77-90, (2005)
12. Z. Nejat, "Effect of Density Ratio on Critical Heat Flux in Closed End Vertical Tube, Int. Multiphase Flow, 7, pp. 321-327, (1981)
13. J. Aharon, I. Hochbaum, Experimental Study of Critical Heat Flux for Low and Zero Flow of Water in Triangle Rod Bundle at Atmospheric Pressure, , The 26th Conference of the Nuclear Societies In Israel, Dead Sea, Israel, (2012)

NOMENCLATURE

A	Flow area
A_H	Heated area
Cw	Constant in Wallis correlation for flooding
D	Tube diameter or characteristic length
D*	Dimensionless tube diameter (D*=D/λ)
G	Mass velocity
G*	Dimensionless mass velocity
h_{fg}	Evaporation heat of the liquid
Δh	Inlet enthalpy subcooling
Ki	Kutateladze number $K_i = j_i \rho_i^{0.5} (g\sigma\Delta\rho)^{-0.25}$ (i=l or i=g for liquid or vapor respectively). C_k and m are
q*	Dimensionless heat flux
q_{cF}*	Dimensionless heat flux due to flooding
λ	Length scale of the Tailor wave
ρ_k	Density of phase k (k=g or l for vapor or liquid)
Δρ	Difference of the density between two phases
P	Pressure
Q	Water flow rate
q"	Heat flux
$q"_{chf}$	Critical heat flux
T_{in}	Inlet temperature
T_{out}	Outlet temperature
T_{osv}	Temperature at OSV
T_{sat}	Saturation temperature
T_w	Wall temperature
v	Velocity
X_e	Exit quality
z	Length coordinate
$(\Delta h_{sub})_i$	Inlet subcooling enthalpy
ΔT_{sub}	Local subcooling ($T_{sat} - T$)